SCIENCE CHINA
Technological Sciences

Special Topic: Flexible Electronics Manufacturing
•Review•

February 2019 Vol.62 No.2: 209–223
https://doi.org/10.1007/s11431-018-9397-5

Flexible and stretchable metal oxide gas sensors for healthcare

ZHENG XiaoQi[1,2] & CHENG HuanYu[1,3*]

[1] *Department of Engineering Science and Mechanics, The Pennsylvania State University, University Park, Pennsylvania 16802, USA;*
[2] *School of Physical Science and Technology, ShanghaiTech University, Shanghai 201210, China;*
[3] *Materials Research Institute, the Pennsylvania State University, University Park, Pennsylvania 16802, USA*

Received August 27, 2018; accepted November 23, 2018; published online December 14, 2018

Capable of measuring volatile biomarker produced by the metabolism from several secretion pathways, flexible and stretchable metal oxide gas sensors have received increasing attention and their development for healthcare starts to gain momentum. Integration of semiconducting metal oxide on a soft, thin, flexible substrate is the key to enable the flexible property to the gas sensor and such integration typically involves either a direct growth or post transfer of the metal oxide on or to the flexible substrate. In addition to the planar plastic substrate, textile represents another important class of flexible substrates due to its ease of integration with clothing. Moreover, the integration of metal oxide on a single fiber provides a great versatility for different applications. Though flexible sensors can easily conform to the developable surface (e.g., cylinder or cone) from a bending deformation, the conformal contact between the sensor and the tissue surface that is often non-developable requires the sensor to be capable of stretching. Due to the intrinsically brittle nature of the semiconducting metal oxide, several stretchable structures have been explored. Despite the great strides made to the burgeoning area of flexible and stretchable metal oxide gas sensors, grand challenges still need to be overcome before the technology can be applied for the practical application. The selected challenges discussed in this mini-review also represent a fraction of possibilities and opportunities for the research community in the future.

metal oxide gas sensor, flexible and stretchable properties, structural design strategies, volatile biomarker

Citation: Zheng X Q, Cheng H Y. Flexible and stretchable metal oxide gas sensors for healthcare. Sci China Tech Sci, 2019, 62: 209–223, https://doi.org/10.1007/s11431-018-9397-5

1 Introduction

Increasing attention has been paid to personal healthcare and human-activity monitoring [1,2]. As an important class in the bio-integrated electronic devices, wearable gas and vapor sensors are being explored to detect gases from the human body and environment for early warning and personal protection [1,3–5]. The volatile biomarker produced by the metabolism has long been known in the medical sciences. The detection of the volatile organic compounds is possible due to several secretion pathways, including breath [6], skin perspiration [7], saliva [8], urine [9,10], and others [11]. Despite the high potential, the continuous monitoring of volatile biomarker has been limited by the challenge of the ultra-low concentration of gas molecules in the complex mixture. Therefore, the design and development of wearable gas and vapor sensors are driven by high sensitivity and selectivity, as well as by low modulus, lightweight, and flexible and stretchable properties of the integrated system.

The gas sensor needs to first recognize the target gas and then convert the recognition event to a measurable signal. Various types of gas sensors have been explored with diverse working principles and methods of integration, resulting in differences between their performances, applicable gas, and occasions. Among the gas sensors that are based on quartz crystal microbalance [12,13], surface and bulk acoustic wave

*Corresponding author (email: huanyu.cheng@psu.edu)

devices [14,15], calorimetric sensors [16], electrochemical cells (e.g., lambda probe [17,18]), and gas-sensitive field-effect transistors [19], chemiresistors have attracted considerable attention in both scientific and practical applications [20,21]. Besides providing real-time changes in their electrical resistance in response to the nearby chemical (gases and vapors) environment, chemiresistors are inexpensive and require just simple DC electronics and small devices suitable for miniaturization [22].

Metal oxides, one representative class of chemiresistors, change their electrical resistance upon interaction with reducing or oxidizing gases. The metal oxide gas sensors are typically associated with short response time, accurate conversion of signals, high sensitivity, reversibility, low-cost manufacturing [22–24], and substantially improved selectivity [25], resulting in extensive studies and widespread applications. The common target gases with their physical properties and threshold values for applications in healthcare are listed in Table 1. Though the list is not exhaustive, this mini-review will focus on the discussion of a few representative examples from this list. Due to the intrinsically brittle nature of metal oxide, it is challenging to implement metal oxide gas sensors in a wearable form. Recent advances in materials and mechanics have provided effective means for the design and fabrication of the flexible and stretchable metal oxide gas sensors. The applications of these novel metal oxide gas sensors also go beyond biomedicine to detecting explosion [26], alarming leakage of gaseous hazards [27,28], monitoring gas emission from vehicles [29,30], and etc. Having addressed several key issues that are directly relevant to the wearable gas sensors [1,2,11,31–34], this new class of wearable devices starts to gain momentum. A brief highlight of the recent studies is provided here to help facilitate further advances in this burgeoning area. In this mini-review, we begin with a brief introduction of the sensing mechanism of the semiconducting metal oxide gas sensors in Section 2. Next, the various strategies and corresponding design considerations of flexible and stretchable metal oxide gas sensors are provided in Section 3 and Section 4, respectively. The review is concluded with a brief discussion on the future perspectives with challenges and potential opportunities for the development of flexible and stretchable metal oxide gas sensors for healthcare.

2 Sensing mechanism of semiconducting metal oxide gas sensors

The working principle of a typical resistive semiconducting metal oxide has been discussed in great detail in several references [40,48,49]; thus, only brief highlights will be provided here. The change in resistance of the sensor material is based on a shift in the equilibrium states of the surface oxygen reaction due to the presence of the target gas analyte. The reducing gas results in an increase of the conductivity for n-type semiconductors and a decrease for p-type semiconductors, whereas the effect of the oxidizing gas is vice versa. For instance, oxygen is ionosorbed on the metal oxide surface in presence of oxygen and absence of any humidity for SnO_2, a wide-bandgap n-type semiconducting material widely used for gas sensing. Acting as electron acceptors, the ionosorbed oxygen species extract electrons to create an electron-depleted surface region (depth of air or the Debye length that is typically on the order of 2–100 nm),

Table 1 List of common target gases measured for applications in healthcare[a)]

Target gases	Physical properties	Threshold values	Applications in healthcare	Ref.
H_2	Colorless, highly flammable, readily forms explosive mixtures with air	20 ppm above basal	Diagnosis of metabolic disorders or diseases	[35,36]
NO_2/NO	Brown gas/colorless, smell like chlorine, poison, oxidizer	206 ppt	Lung injury	[37,38]
CO	Colorless, odorless, toxicity	0.1 ppm	Diagnosis of hemolytic disease	[39,40]
CO_2	Colorless, odorless at low concentration	60 ppb	Respiration monitoring	[41]
H_2S	Colorless, rotten eggs smell, flammable and highly toxic	534 ppt	Asthma, diagnosis of halitosis and lung cancer	[37]
NH_3	Colorless, strong pungent odor, flammable	10–50 ppb	Liver failure	[42,43]
C_2H_5OH	Colorless, alcoholic smell and taste, flammable, low toxicity	0.1 ng	Alcohol consumption	[44,45]
C_3H_6O	Colorless, pungent odor, sweetish taste, flammable	10–30 ppb	Hyperglycemia, diabetes	[7,46,47]
Methane	Colorless, odorless, nontoxic yet extremely flammable	20 ppm above basal	Indicating lactose intolerance	[35]

a) H_2: Hydrogen; NO_2/NO: Nitrogen dioxide; CO: Carbon monoxide; CO_2: Carbon dioxide; H_2S: Hydrogen sulfide; NH_3: Ammonia; C_2H_5OH: Ethanol; C_3H_6O: Acetone

with a maximum surface coverage of about 10^{-3} cm^{-1} to 10^{-2} cm^{-1} ions as dictated by the Weisz limitation [50]. Band bending owing to the negative surface charge generates a surface potential barrier of 0.5 eV to 1.0 eV. Both of the depth and height of the barrier depend on the amount and type of the adsorbed oxygen. In polycrystalline material, the electrical conductivity occurs along the percolation path via the grain-to-grain contact, which depends on the height of the surface potential barrier (or the Schottky barrier) $eV_{surface}$ between the adjacent grains. The conductance G can be related to the Schottky barrier as $G \approx \exp[-eV_{surface}/(k_BT)]$ [51]. Reacting with the ionosorbed oxygen species, the reducing gases (e.g., H_2, H_2S, CO, NH_3, CH_4, ethanol, acetone) decrease the adsorbed oxygen to release the surface-trapped electrons back to the bulk. As a result, the reduced Schottky barrier increases the conductance of the sensing material. In contrast, the oxidizing gases (e.g., O_2, O_3, NO_x, CO_2, or SO_2) further extract electrons from the semiconductor, resulting in an increased Schottky barrier and thus a decrease in the conductance. For metal oxide in the shape of a nanosized particle, both experimental observation and theoretical evidence indicate a smaller a particle, a higher sensitivity of the sensing material. This is attributed to the fact that the nanostructure dimensions allow the entirety of the sensing materials to be within the Debye length and depleted by the gas analyte for the maximum response. However, the surface accessibility for the exposed gas to the metal oxide depends largely on the tailored properties of the sensing material, which may still include empirical approaches.

Although metal oxide gas sensors are associated with high sensitivity, low cost, and compatibility with modern electronic devices as mentioned above, their relatively poor selectivity among gases makes them impossible to use a single sensor to identify a specific gas from a mixture. One straightforward method is to exploit a suite of coordinated sensors to simultaneously analyze the signals from the array of sensors, often termed as electronic noses [52]. In order to simplify the design in the electronic nose, a separate effort is to use composite metal oxides for enhanced selectivity. Combining two dissimilar materials with a heterojunction at the physical interface can result in a heterostructure. An extensive review has discussed the heterostructure from binary compounds [53] and highlights are briefly reviewed here. Various classes of heterostructures have been achieved through (1) a simple mixture of two constitutes, (2) adding a second oxide on the base metal oxide (e.g., sputtering), and (3) a well-defined partition or interface between two oxides. When analyzing the behavior of the heterostructure for gas sensing, a heterojunction that modulates the sensing property through the p-n junction is a very common interface. In direct contrast to the most commonly used pure n-type gas sensors, the electrons at the higher energy states at the interface in the heterostructure will flow to unoccupied lower energy states (i.e. 'Fermi level-mediated charge transfer') to create a depletion region at the interface. This results in a potential energy barrier due to band bending that the electrons must overcome.

As the adsorption of the oxygen and reaction rates of the analyte gas are temperature dependent, an optimum operating temperature often exists (termed as working temperature) and designs that ensure highly uniform temperature distribution are also desirable [32]. For an n-type sensing material, the response is typically defined as the ratio of the electrical resistance in the presence of a gas to that in the air (R_{gas}/R_{air}) for an oxidizing gas and R_{air}/R_{gas} for a reducing gas. Plotting the response of the sensor as a function of the gas concentration yields a calibration curve of the sensor, from which the calculated slope defines the sensitivity. The response (or recovery) time is typically defined as the time the sensor takes to reach 90% of its steady-state value upon the introduction (or removal) of the analyte gas.

3 Flexible metal oxide gas sensors

Due to the geometry mismatch between a flat gas sensor and the curvilinear surface of the human body, a wearable gas sensor is required to be capable of bending. As a structure's bending stiffness typically scales with the cubic of its thickness, reduction in thickness of the structure can significantly decrease its resistance against bending formation. Because the metal oxide gas sensor itself is already thin in its thickness, it is highly desirable to integrate the gas sensor on a thin substrate. Taken together with the fact that the reduced Young's modulus of the substrate can approximately decrease its bending stiffness in a linear manner, a class of soft polymers has been explored as the substrate for the wearable gas sensors, including polyethylene terephthalate (PET), polyimide (PI), polydimethylsiloxane (PDMS) and polyethylene naphthalate (PEN) [54]. Direct growth and post-transfer are the two commonly used strategies for the integration of metal oxide gas sensor on a flexible substrate.

3.1 Direct growth of metal oxide on flexible substrates

To directly grow metal oxide materials on a flexible substrate, the processing temperatures are required to be below the glass transition or thermal degradation temperatures of the flexible substrate [55]. As an example, the single-crystalline ZnO nanowires (NWs) can grow at 80°C via electrodeposition on a transparent PET substrate coated with a patterned indium-tin-oxide (ITO) layer [56]. In a similar approach, thermolysis assisted chemical solution method is used to continuously grow ZnO nanorods on a PI film covered by an 80 nm thick ZnO seed layer from radio-frequency (RF) sputtering [57]. The flexible ZnO nanorod sensors de-

monstrate the sensing performance of ethanol in a range of 10–100 ppm comparable with those fabricated on a rigid silicon dioxide substrate. Moreover, the rapid hydrothermal synthesis through the use of the variable power microwave sintering system can be used to synthesize undoped ZnO NW arrays and Al-doped ZnO nanostructures (e.g., nanowires and nanosheets) on PET [58].

In addition to the plastic substrate with a thin geometry, the paper is also associated with a cost-effective manufacturing process and a high surface-to-volume ratio due to its hierarchical structure [55], suggesting it as a promising flexible substrate. When compared with the plastic substrate, however, a much lower temperature should be used for the synthesis of the metal oxide. Exploiting low-temperature (i.e., 85 and 90°C) hydrothermal technique allows the direct growth of vertically aligned single crystalline ZnO nanorods and nanoneedles on a paper substrate [59]. As a result, fabrication techniques of metal oxide gas sensors on paper substrates and the influence of paper type on sensing performance have been explored in several studies [44,60,61]. On the top surface of a flexible cellulose glossy paper substrate, a custom-built tool is used to deposit conductive carbon nanotubes as interdigitated electrodes, followed by a sensing material with ITO nanopowders dispersed in a polydiallyldimethylammonium chloride (PDDAC) polymer matrix [44] (Figure 1(a)). Because none of the two components in the sensing material shows a response to ethanol in the experimental condition, the capability of the sensor to detect low concentration of ethanol at room temperature is attributed to the electrostatic interaction between negatively charged ITO particles and positively charged polymer (Figure 1(b)).

Successful growth of one metal oxide such as ZnO nanorods provides a platform for adding a metal catalyst or a second metal oxide layer. As an example, Ag nanoparticles are sputter coated on the as-grown ZnO nanorods that are synthesized on a PI layer pasted onto a polytetrafluoroethylene (PTFE) sheet [54] (Figure 1(c)). With catalytic activities of Ag, the fabricated sensor demonstrates a high response of 27.2, short response (recovery) time of 62 s (39 s) to acetylene at 1000 ppm, and a broad detection range from 3 to 1000 ppm at a low operating temperature of 200°C (Figure 1(d)). Tests of mechanical flexibility and reliability further show a negligible drift of 2.1% for a maximum bending angle of 90° and a decrease of 8% in response after 5×10^4 bending/relaxing cycles. In another similar effort to design flexible H_2 sensor [26] (Figure 1(e)), ZnO nanorods are still synthesized on a PI layer attached to a Si substrate. After sputter coating Pd nanoparticles on the as-grown ZnO, the sample is detached from the Si substrate and transferred to a PET substrate for gas sensing and mechanical testing. Upon bending, the sensor even shows an improved response possibly due to a higher surface reactivity from bending for more gas adsorption. Stable sensor response is also observed after 10^5 bending/relaxing cycles (Figure 1(f)). When a free-standing, thin graphene/metal sheet is used as a top electrode on vertically grown ZnO nanorods, the ethanol gas sensor itself can be made into a transparent form with good transmittance over the range of visible light [62].

Growing a second metal oxide on the first creates a metal oxide heterostructure with a heterojunction. Coating In_2O_3 nanoparticles on vertically aligned ZnO NW by a simple wet-chemical method yields core-shell In_2O_3/ZnO heterostructure on a Ti foil [63] (Figure 1(g) and (h)). In comparison to the bare ZnO NW array, the heterostructure conversion of In_2O_3/ZnO to In_2S_3/ZnO upon exposure to H_2S changes the electron depletion layer on the ZnO surface to an accumulation layer, resulting in a stronger free-carrier piezo-screening effect than that of gas adsorption of H_2S. In addition, the In_2O_3/ZnO nanoarray nanogenerator can piezoelectric output power as an energy source, providing an important step toward the self-powered active gas sensor. The heterostructure can also form between a metal oxide and other gas sensing materials such as a conducting polymer. In addition, the other techniques can be explored for the synthesis of metal oxide. In an effort to form a polyaniline@SnO_2 heterojunction on a flexible PET [64], a SnO_2 precursor solution is electrospun and calcinated to form SnO_2 nanofibers first. Immersing a piece of pretreated PET film with a mixed solution of aniline monomer in HCl and ammonium persulfate (APS) as an oxidant in ice water in a mass ratio of 1:1 yields polyaniline via an *in situ* oxidative polymerization method. Simple coating with different amounts of SnO_2 followed by another immersion for polymerization completes the process for PANI-SnO_2 hybrid composites. The hybrid NH_3 sensors show significantly enhanced sensitivity over their constituent components at room temperature (i.e., 5 times and 29 times higher than PANI and SnO_2). This enhancement is partially due to the improved interaction between NH_3 and N^+-H sites of PANI, but is mainly attributed to the formation of the p-n heterojunction between the organic p-type PANI and the inorganic n-type SnO_2.

In addition to ZnO that is mostly reported owing to its good gas sensing performance and biocompatibility [65], several other metal oxides are also studied, including CuO [66,67], SnO_2 [45,68], MoO_3 [69], WO_3 [61,70], TiO_2 [71,72], and etc. A thin layer of Cu sputtered on Kapton substrates with a possibility to pattern through shadow masks can be thermally oxidized to form p-type CuO NWs to detect ethanol and methane of 50 ppm at a working temperature of 400°C (or appreciable response towards CO, H_2, acetone, H_2S, and O_3) [66]. In-plane tensile stresses may also be used during the oxidation process of Cu to effectively promote the CuO NW formation with significantly increased density [67]. Following the synthesis of flower-like WO_3 nanostructure material, an *in situ* chemical oxidation polymeriza-

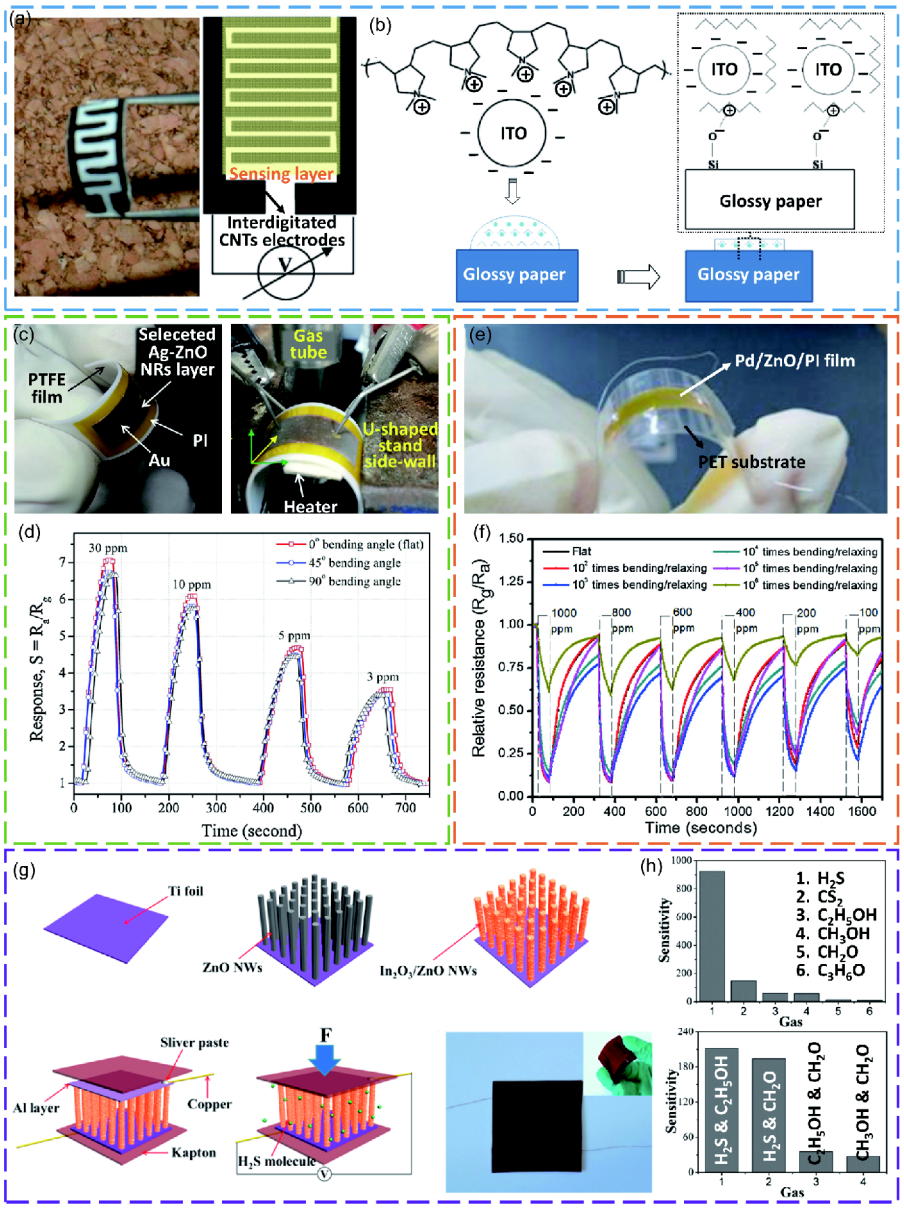

Figure 1 (Color online) **(a)** Optical image and schematic illustration of a fabricated flexible ethanol sensor with the interdigitated electrodes deposited on a glossy paper; **(b)** schematic illustration of the ethanol sensing enhancement due to the electrostatic interaction between the poly-diallyldimethylammonium chloride (PDDAC) and indium-tin-oxide (ITO) nanopowders. (a)–(b): adapted with permission from ref. [44]. Copyright 2010 by Elsevier; (c) photographs of the acetylene gas sensor and its testing apparatus; (d) responses under different bending angles toward 3 ppm to 30 ppm acetylene at 200°C. (c)–(d): reproduced with permission from ref. [54]. Copyright 2016 by Elsevier; (e) optical image and (f) stability with different bending/relaxing cycles of the hydrogen gas sensor. No significant loss of performance before 10^6 cycles. Reproduced with permission from ref. [26]. Copyright 2013 by Elsevier; (g) the schematic illustration that shows the fabrication process of the self-powered gas sensor based on In_2O_3/ZnO core-shell heterostructure (inset shows an optical image of the bent device); (h) Selectivity and sensitivity toward different gases (700 ppm for single gases and 350 ppm+350 ppm for mixed gases). (g)–(h): reproduced with permission from ref. [62]. Copyright 2014 by American Chemical Society.

tion method is used to prepare Polyaniline (PANI)@flower-like WO_3 nanocomposites on a flexible PET substrate with interdigitated electrodes [73]. Owing to the formation of the p-n heterojunction at the interface between PANI and flower-like WO_3, the NH_3 sensor exhibits low detection limit of 500 ppb, rapid response and recovery rates, and outstanding selectivity at room temperature, as well as good moisture resistance. In order to form highly aligned TiO_2 and Nb-doped TiO_2 nanotubes on flexible substrates for a CO gas sensor, electrochemical anodization of Ti and Ti–Nb films sputtered on a Kapton film is used as a low cost and convenient method [74,75]. Other than a chemoresistive gas sensor, the TiO_2 and Nb–TiO_2 nanotubular structures formed on the flexible substrate can also be used for flexible dye-sensitized solar

cells and other applications.

3.2 Post-transfer of metal oxide onto flexible substrates

As the typical processing temperatures of metal oxides are relatively high, the direct growth on a flexible substrate is limited to a certain class of metal oxides. In order to explore a wide range of metal oxides, a transfer process has been exploited to transfer the metal oxide that is synthesized on rigid substrates to the flexible substrate. Various approaches have been developed for the transfer of inorganic semiconducting materials to mechanically flexible substrates [76–79]. A typical transfer process involves the use of a sacrificial layer in the initial growth step. For example, the vertical carbon nanotubes (CNTs)/reduced graphene hybrid film that is first grown on a SiO_2 layer supported on a Si wafer can be detached from the Si substrate by etching the SiO_2 sacrificial layer in a dilute HF solution, followed by a transfer to an Au/polyimide flexible substrate [80]. In comparison to the reduce graphene, the hybrid film exhibits remarkably enhanced sensitivity to NO_2 gas with weak n-p transitions. The slow recovery is also addressed by embedding a Ni/Cu microheater in the polyimide substrate to promote desorption of the NO_2 gas molecules. Due to the use of the flexible polyimide substrate and the reduced graphene thin film, the gas sensor can bend over a radius of 15 mm to detect the presence of 5 ppm NO_2. Careful choice of the growth substrate may also eliminate the use of a sacrificial layer. Due to the weak adhesion between an ultrathin (1.9 μm) poly(methyl methacrylate) (PMMA) layer and a glass slide, palladium (Pd)-decorated indium-gallium-zinc oxide (IGZO) H_2 sensor fabricated on the PMMA substrate can be readily peeled off the underlying unmodified glass slide [81]. The PMMA substrate with the H_2 gas sensor can then attach to nonplanar substrates such as poly (vinyl chloride) (PVC) gas tubes (Figure 2(a)) or wrinkled hand gloves (Figure 2(b)), demonstrating an excellent sensitivity at room temperature without performance degradation even at a bending radius down to <1 mm (Figure 2(c) and (d)).

Drop-casting is a simple yet effective means to transfer dispersion of sensing materials that are synthesized from a process with a relatively high temperature onto the flexible substrates. For instance, an ethanol sensor results from drop-casting of commercial ZnO nanoparticles in deionized (DI) water on a PET-ITO layer in a parallel electrodes geometry, followed by evaporation of DI water at 70°C for 2 h [82] (Figure 2(e) and (f)). As the UV irradiation generates high-density free carriers and highly reactive photo-induced oxygen ions, the sensor shows a relatively high response to ethanol even at room temperature. The use of the PET-ITO substrate also shows a transmittance of more than 62% over the visible spectrum range and allows sensing upon bending over a radius of 3.5 mm. In a similar approach, depositing a mixture of SnO_2 nanopowder and PDDAC on a PI substrate with interdigitated electrodes results in an ethanol sensor that can detect 10 ppm at room temperature [45]. In addition to the use of commercial nanoparticles, inks with heterostructures can be prepared for the use of drop-casting. After infiltration and reduction of Pd nanoparticles into the cavity of the Co-based metal-organic framework (MOF, e.g., ZIF-67), a calcination process at 400°C for 1 h results in the formation of PdO-Co_3O_4 hollow nanocubes (PdO-Co_3O_4 HNCs) [83]. Mixing PdO-Co_3O_4 HNCs with SWCNTs increases the conductivity of the sensing material. Drop-casting the SWCNTs-loaded PdO-Co_3O_4 HNCs inks on a high-temperature-resistant colorless PI with an interdigitated electrode on top and a flexible heater that embeds Au-covered Ni mesh on back generates a flexible NO_2 gas sensor (Figure 2(g)). At elevated operation temperature, the sensor shows improved reaction kinetics, enhanced sensitivity, and a low detection limit for the NO_2 sensing (Figure 2(h)). Moreover, the integrated sensor with a flexible heater exhibits a high mechanical stability with negligible baseline resistance drift over 4000 cyclic bending cycles. Similar to drop casting, gel casting can also be used to disperse the sensing material onto the flexible substrate. With the assistance of α-terpineol, hydrothermally synthesized WO_3 nanoparticles can mix with commercial MWCNTs to form a viscous gel of MWCNTs-WO_3 hybrid [70]. Gel casting the MWCNTs-WO_3 hybrid between two Au electrodes separated by 1 cm on a PET substrate yields a flexible sensor with excellent selectivity to NO_2 at room temperature and mechanical robustness over 10^8 bending/relaxing cycles.

The technique to transfer printing gas sensing materials from the growth substrate to the target flexible substrate can also be applied to the other materials. Through the use of a PDMS stamp, ultrahigh-density, highly aligned arrays of silicon NWs are picked up from the silicon-on-insulator substrate and then printed onto a plastic substrate to yield field-effect transistors with parts-per-billion sensitivity to NO_2 [84]. By constructing an array of sensors, the system has demonstrated the capability to distinguish low concentration (1000 ppm) of acetone from hexane solvent vapors. In the specific case of inorganic NWs, aligned assembly techniques also include flow-assisted [85–87], Langmuir–Blodgett [88–90], bubble-blown [91], electric-field-directed assembly [92,93], contact printing [94–96], and nanoscale combing [97]. A change of the stamp from PDMS to a thermal release tape that modulates the adhesion can also be used for transfer printing of aligned nanotubes onto flexible substrates [98]. These techniques have provided a versatile platform for integrating gas sensors on flexible substrates [34,55,99,100].

3.3 Integration of metal oxide with textile

Besides flat thin films discussed in the above sections, fab-

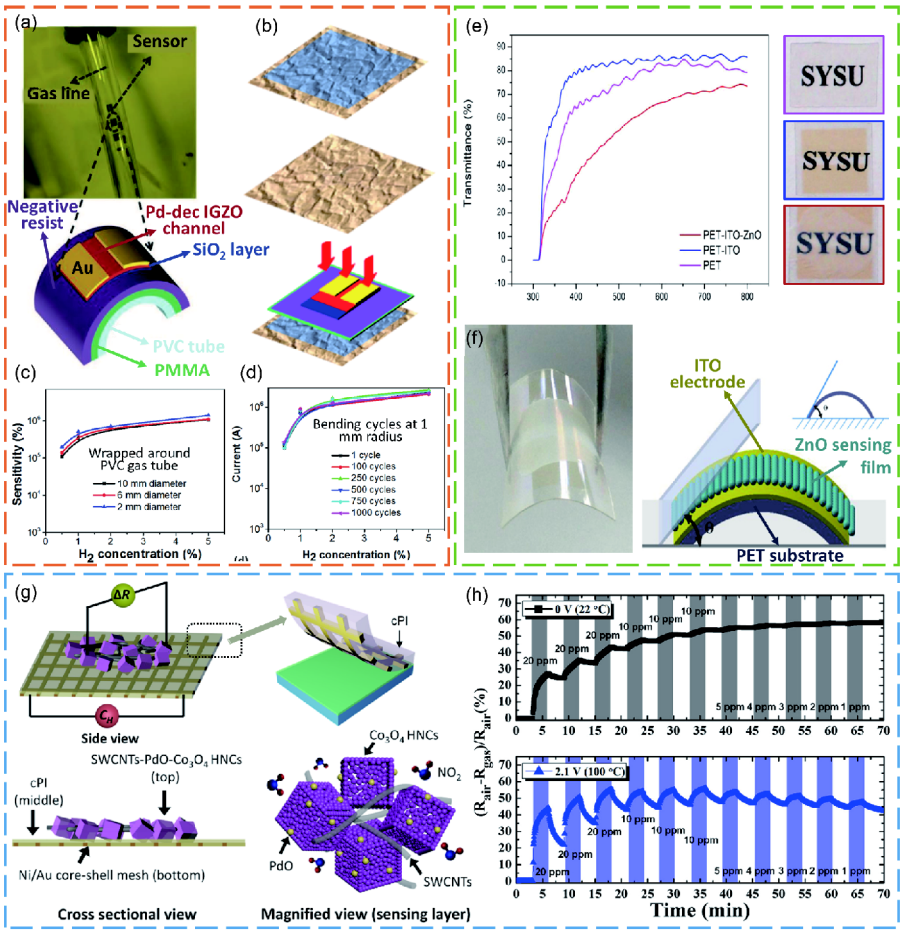

Figure 2 (Color online) (a) Optical image and schematic that show the structure and attachment of the Pd-decorated IGZO-based H_2 sensor to a PVC gas tube; (b) the ultra-thin geometry of the PMMA allows attachment of the gas sensor on a wrinkled hand glove, which includes the steps of coating photocurable polymer and UV exposure; (c) sensitivities with different bending diameters; (d) Stability test at a bending radius of 1 mm. (a)–(d): reproduced with permission from ref. [81]. Copyright 2018 by John Wiley and Sons; (e) the measured transmittance over the visible wavelength and corresponding optical images of PET, PET-ITO substrates, and PET-ITO-ZnO gas sensor, respectively; (f) optical image and schematic illustration of the flexible and transparent ethanol gas sensor. The curvature angles of 61.65° and 90° correspond to the bending radii of 5.12 mm and 3.5 mm, respectively. (e)–(f): reproduced with permission from ref. [82], which is used under CC BY 4.0; (g) schematic illustration of the SWCNTs-PdO-Co_3O_4 hollow nanocubes on a colorless polyimide layer embedding a Ni/Au core-shell mesh electrode at the back surface; (h) sensitivity upon exposure toward NO_2 under an applied voltage of 0 V and 2.1 V, corresponding to 22°C and 100 °C, respectively. (g)–(h): reproduced with permission from ref. [83]. Copyright 2017 by American Chemical Society.

rics and smart textiles have started to gain momentum in the development of flexible gas sensor due to their intrinsically flexible properties, ease of integration with clothing, and possible demonstration for fashion [103]. The metal oxide gas sensor could be integrated on the fabric or a single fiber. The process for the former is similar to the use of the other flat thin films. The low-temperature hydrothermal method also allows the direct growth of ZnO nanorods on a typical fabric lab-coat and the room temperature response of the sensor to H_2 gas demonstrates an electrical resistance change of 27% after 10 min exposure of 1000 ppm H_2 (or 83% with a sputtered ~5 nm thick catalytic Pt layer) [101] (Figure 3(a) and (b)). This ready-to-wear ZnO nanorods device is robust against mechanical deformation and washing cycles, providing a cost-effective manufacturing route for the wearable gas sensor. In another example, the surface of the cotton fabric is modified with ZnO nanostructures by sputtering of the seed layer and sol-gel growth of ZnO [103]. The functionalized cotton fabric shows room temperature gas-sensing of volatile organic compounds (e.g., acetaldehyde, ammonia, and ethanol), as well as an excellent UV filtering capability with enhanced ultraviolet protection factor against UV radiation. The metal oxide sensing material can also be prepared in a fiber mat geometry for a flexible property. Without the need to worry about substrate damage, SnO_2 polycrystalline nanofibers doped with MWCNTs synthesized through electrospinning can be followed by a calcination process at 500°C in the air [104]. Due to the increased binding energy between multiwall carbon nanotubes (MWCNTs) and carbon monoxide (CO) and thereby large electron charge transfer from MWCNTs to CO, the resulting MWCNTs-SnO_2 sensors are capable of detecting CO of

50 ppm at the room temperature. The demonstrated MWCNT doped SnO_2 nanofiber mats have the potential for wearable room temperature gas sensors for their flexible geometry and low-cost manufacturing method.

In comparison to the fabric substrate, the integration of metal oxide on a single fiber offers a great versatility, but it also involves additional challenges bending, twisting, or stretching in the weaving process. Electrodeposition of zinc on a carbon microfiber textile followed by a thermal oxidation yields a hierarchic nano-on-micro ZnO NW structure with a high surface-to-volume ratio [105]. The idea of integrating metal oxide on a single fiber/yarn can also be extended to create the sensor in a fiber geometry. Aligned MWCNTs sheets drop cast with prefabricated metal-organic frameworks (MOFs) (e.g., ZIF-67-Co and MIL-88-Fe) can be twisted with a motor into a desirably aligned MOF/MWCNT hybrid fiber [31]. Following heat treatment such as annealing at 300°C for 2 h in air, ZIF-67-Co in the hybrid fiber transforms into Co-based oxide (i.e., Co_3O_4). Similarly, annealing MIL-88-Fe/MWCNT in air yields Fe_2O_3/MWCNT hybrid fiber (Figure 3(c) and (d)). The Co_3O_4/MWCNT hybrid fiber demonstrates remarkable sensitivity to measure NO_2 down to 0.1 ppm at room temperature and (Figure 3(e) and (f)). A better response in the Co_3O_4/MWCNT hybrid fiber sensor is observed upon bending (Figure 3(g)) and it is attributed to the improved electron transfer along the radial direction from the partially straightened fiber due to the tensile strain. Sewing the hybrid fiber into the commercially available textile fabric also demonstrates the easy integration and mechanical robustness of the hybrid fiber. In addition, the hybrid fiber can also serve as a supercapacitor to store energy for wearable devices. It should also be noted that the smart textile is also compatible with the electronic nose design [102] (Figure 3(h)).

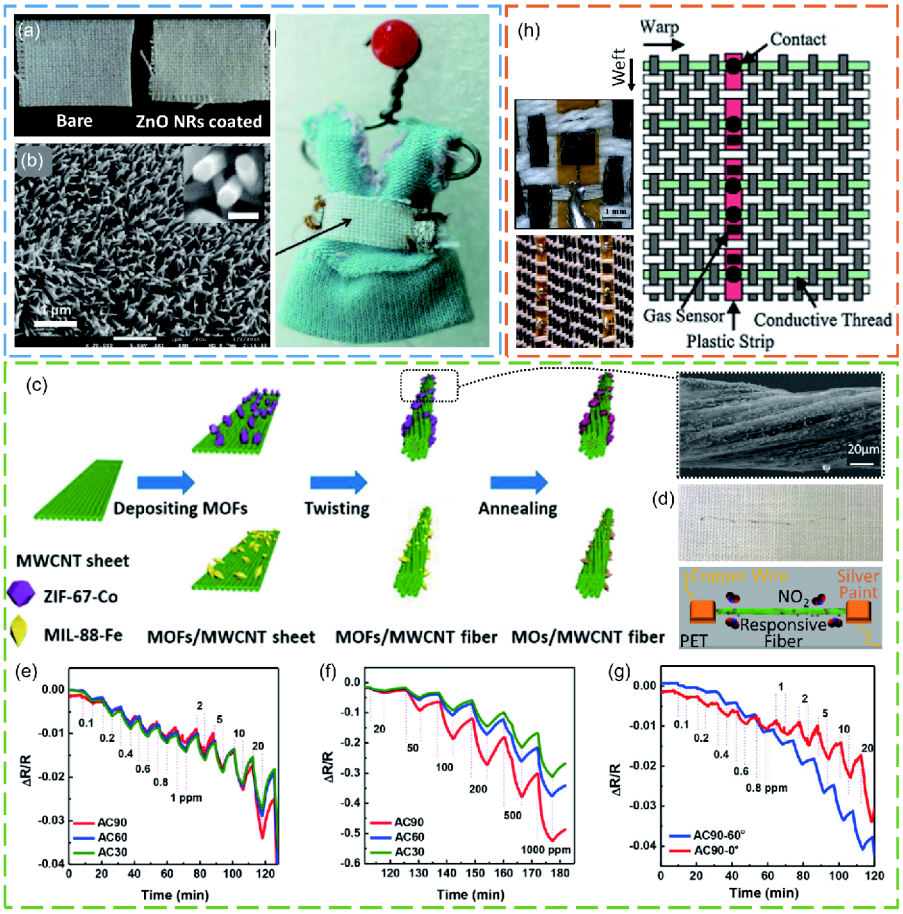

Figure 3 (Color online) (a) Optical images of bare and ZnO nanorod-coated cotton fabric; (b) SEM and optical images of ready-to-wear ZnO nanorods hydrogen gas sensor. (a)–(b): reproduced with permission from ref. [101]. Copyright 2010 by Elsevier; (c) the schematic illustration that shows the fabrication process of metal oxides/MWCNT hybrid fiber gas sensor and the inset shows the SEM image of ZIF-67-Co/MWCNT hybrid fiber; (d) optical image of a hybrid fiber woven into a lab coat and schematic illustration of the hybrid fiber sensor used for NO_2 detection; normalized responses of Co_3O_4/MWCNT hybrid fiber with different Co_3O_4 loadings to NO_2 in the concentration ranges of (e) [0.1, 20] ppm and (f) [20, 1000] ppm (AC30 indicates 30 wt% of ZIF-67-Co loading, followed by an annealing process); (g) responses of Co_3O_4/MWCNT hybrid fiber (AC90) with and without bending under different concentrations of NO_2. (c)–(g): reproduced with permission from ref. [31]. Copyright 2018 by American Chemical Society; (h) schematic diagram and photograph of a novel electronic nose design in a woven textile band and one enlarged gas sensor (upper left). Reproduced with permission from ref. [102]. Copyright 2012 by Elsevier.

4 Metal oxide gas sensors integration with stretchable substrates

It is highly desirable for the wearable metal oxide gas sensor to have a conformal contact with the skin of the human body. The capability to bend allows a flat geometry to form conformal contact with a developable surface (Gaussian curvature of zero such as cylinder or cone). For the non-developable surface, the stretchable property would be essential to form a conformal contact. To enable the stretchable property to the intrinsically rigid metal oxide, structural design strategies have been explored [106–109]. A wavy geometry of the metal oxide created by the use of pre-strain strategy can allow it to be stretched flat and the small strain in the wavy metal oxide is directly related to the applied tensile strain [110–112]. Instead of creating wavy metal oxide, a flat metal oxide can also be connected by wavy metallic interconnections by adopting the previous established "island-bridge" layout [113–115]. Selectively bonding the metal oxide to a stretchable substrate with a surface relief structure isolates the strain to the region of wavy interconnection [116–119]. Other structural design strategies include interconnected cracks [120,121], 2D/3D helices [122,123], origami/kirigami [124–127], and interlocks [128,129].

As a simple yet effective strategy, pre-strain has been widely used to create stretchable structures. In a recent study [130], graphene electrodes and colloidal PbS quantum dots sensing layer are first transferred to a pre-strained elastomeric substrate via dry transfer and spin-coating, respectively (Figure 4(a)). The release of the pre-strain results in an stretchable gas sensor in a wavy geometry. Owing to the anti-humidity interference ability of the colloidal PbS quantum dots, the sensor demonstrates an improved humidity resistance, as well as a high sensitivity in response to NO_2 at room temperature even under 1000 stretch/relax cycles. In addition, the wavy gas sensor exhibits a much smaller variation in the NO_2 detection from a relative humidity of 0% to 86.7% when compared with the flat gas sensor. Due to the great solution processability of colloidal quantum dots, those based on a metal oxide such as SnO_2 can be expected to create stretchable gas sensors with enhanced catalytic activity and fast response to H_2S [131] (Figure 4(b)).

Apart from the pre-strain strategy, the island-bridge design can also be used to provide a stretchable system, where the rigid sensors are placed on the island region interconnected by deformable bridges. In a multisensor system, an MWNT/SnO_2 NW NO_2 gas and UV sensor is integrated with a fragmentized graphene foam strain sensor, an array of nine micro-supercapacitors, and a rechargeable wireless radio frequency power receiver all on a stretchable Ecoflex substrate with an embedded liquid metal interconnection [132] (Figure 4(c)). As validated by the experimental demonstration, the prediction from finite element analysis shows that the strain in the relatively rigid island region is much smaller than that of the deformable bridge region upon an applied tensile strain. The stretchable multisensor system attached to the skin could detect various signals with direct relevance to healthcare, including neck pulse, saliva swallowing, voice, body motion, and sensing of NO_2 gas and UV light signal even under a uniaxial strain up to 50% (Figure 4(d)).

Interconnected cracks can be created from multiple approaches and the resulting metal oxide sensing element itself is stretchable. The integration of metal oxide on an elastomeric polymer can be achieved by a platinum transfer technique [135]. Relying on a weak adhesion between the platinum and Si wafer, the Pt with a metal oxide such as ZnO deposited on top can be removed from the Si wafer by casting a PDMS layer on the ZnO layer. Following a reactive ion etching to remove Pt, ZnO in plate-like micro-cracking structures with overlapping edges are left on the PDMS layer. Due to the strong adhesion between ZnO and PDMS, the structure of tectonic plates in ZnO provides an electrical conduction path upon stretching. The transparent and stretchable ZnO film has been shown to result in enhanced gas sensing performance when compared with their rigid counterparts under room temperature conditions [133] (Figure 4(e)–(g)). In addition to a gas sensor for detection of H_2 and NO_2 gases, the metal oxide on PDMS can also be exploited to create ultraviolet light sensors and a tunable diffraction grating for displacement sensing with nanometer accuracy. This approach also allows the creation of electronic devices with patterns in nanometer resolution over a large area.

In addition to the interconnected cracks, the metal oxide itself can be made stretchable by a simple and versatile flame transport synthesis method [136]. As opposed to the purely diffusion-based approaches such as ALD, the flame-transport-synthesis that is based on convection-driven control of the reaction environment allows a faster reaction rate and thereby a significantly enhanced throughput. The resulting interconnected 3D SnO_2 NW network is used for ethanol sensing and UV detection at room and low temperatures (down to 25 K) [137]. Enabling flexible and stretchable properties to brittle materials, the 3D network from this approach can go beyond the sensing to many other applications, including battery electrode, biomedical, and 3D template for growth of new materials [136,138,139].

It should also be noted that several other strategies can also be exploited for stretchable gas sensors though it is not included in the current demonstration. For example, polyurethane (PU) fibers soak-coated with ZnO seed layer, followed by a hydrothermal reaction, yields a multifunctional ZnO NWs@PU [134] (Figure 4(h) and (j)). Owing to the intrinsically stretchable nature of PU fibers, applied tensile strain creates cracks in the ZnO NW array to

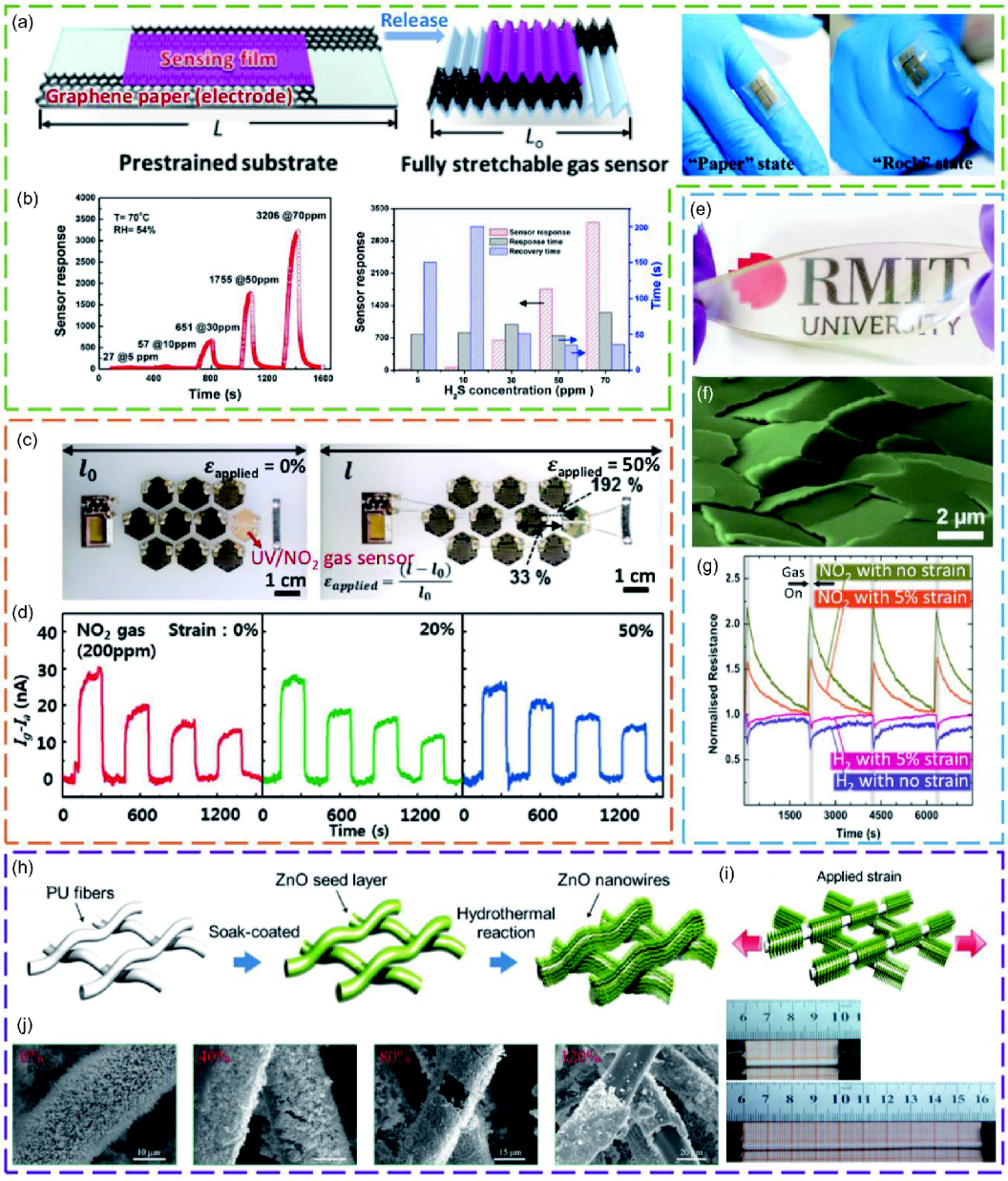

Figure 4 (Color online) (a) A wavy, stretchable quantum dot gas sensor created from the pre-strain strategy (left) and optical images of the gas sensor attached to the finger joint in "paper" and "rock" states (right). Reproduced with permission from ref. [130]. Copyright 2018 by American Chemical Society; (b) responses of the SnO_2 quantum dot gas sensor toward different concentration of H_2S. Reproduced with permission from ref. [131]. Copyright 2018 by Elsevier; (c) photograph and strain analysis of the multisensory system; (d) responses of the NO_2 gas sensor under different strains. (c)–(d): reproduced with permission from ref. [132]. Copyright 2015 by John Wiley and Sons; (e) an optical image that shows the transparent ZnO-based gas sensor is capable of flexing and twisting; (f) SEM image that shows the surface morphology of ZnO in false color; (g) responses toward H_2 and NO_2 with and without stretching at room temperature. (e)–(g): reproduced with permission from ref. [133]. Copyright 2015 by John Wiley and Sons; (h) schematic illustration of the fabrication process of the multifunctional sensor; (i) schematic (up) and photographic (down) illustrations of the sensor under an applied tensile strain; (j) SEM images of the sensor under different applied tensile strains. (h)–(j): Reproduced with permission from ref. [134]. Copyright 2016 by John Wiley and Sons.

result in a percolating pathway. The stretchable network is capable of detecting strain, temperature, and UV. Its potential use for gas sensing can also be envisioned.

5 Conclusion and future perspectives

Aiming to provide only a glance at the recent advances in the burgeoning area of flexible and stretchable metal oxide gas sensors for healthcare, the review here is by no means an exhaustive list. As briefly discussed in this mini-review, great stride has been made. In order to achieve the desired flexible property, the metal oxide sensing material is either directly grown or post transferred to a soft, thin, and flexible substrate. As for the goal to achieve a conformal contact between the bio-integrated metal oxide gas sensor and the

soft tissue, several stretchable structures have been explored. Despite the recent progress, a few challenges still need to be addressed for the practical application.

In order to avoid the adverse thermal effect on the human body and to lower the power budget for long-term operation, it is highly desirable for the wearable metal oxide gas sensor to operate at room temperature. Thus, novel materials and/or heterostructures that provide room-temperature sensing capabilities represent a strong focus for future research. Moreover, the room-temperature processing of the gas sensor is also of interest. For instance, combining a PbS colloidal quantum dots (CQDs) with flexible substrates yields a highly sensitive and fully recoverable NO_2 gas sensor at room temperature [140]. Owing to the large surface area and room-temperature solution processing capability onto various substrates, CQDs that provide tunable binding energy to target gases are promising in wearable gas sensing toward healthcare applications. Anchoring SnO_2 quantum wires on reduced graphene oxide nanosheets by a one-step colloidal synthesis without further sintering results in a sensitive and selective room-temperature H_2S gas sensor [141]. The favorable electron transfer across the interface of the composites could also enhance the room-temperature sensing performance. On a separate route to eliminate the need for an external heater, self-heating is exploited to harness the dissipated power at individual NWs by Joule effect upon application of a biased current [142,143]. With reduced thermal inertia, a single SnO_2 NW only requires few mW (from energy harvesting technologies such as thermoelectric microgenerators) to bias, heat, and measure CO and NO_2, with nearly identical responses to those obtained with integrated microheaters. Similar to the role as an activation energy from the heat, high-density power light energy in the range of the energy gap of the semiconductor has also been used to enable room-temperature sensing. Examples include the detection of NO_2 with SnO_2 [144–146], CO and NO_2 with In_2O_3 and SnO_2 (with or without catalyst/doping) [147,148], or acetone/acetaldehyde/volatiles with nanoparticulate ZnO [149].

A strain in the metal oxide, even small and limited due to the brittle nature of the semiconducting metal oxide, may still change the signal outputs in the sensing material upon mechanical strains [2,106,107]. Depending on the architecture design of the device and especially the position of the sensing material, the sensing material layer may experience in-plane tensile, compressive, or zero strain upon a bending deformation [67]. Such bending-induced strain would alter the microstructure and transport characteristics of carriers in the semiconducting metal oxide sensing layers, therefore affecting the sensing performance. Though the sensitivity of the sensing material is observed to remain unaffected or even promoted in certain cases [54,81,82,133], the lack of qualitative analysis still leaves the strain effect on the gas sensing performance yet to be explored. The change in the signal outputs may also be a combined effect in the presences of target gas and mechanical deformation. Thus, such coupling should be closely examined and a strategy to decouple the different effects will be of an important interest. In an attempt to address this issue, channel transconductance and its equivalent voltage of a field-effect transistor are measured as temperature and pressure are applied, from which a characteristic matrix can be solved [150]. By using the inverse of the characteristic matrix, both temperature and pressure can be determined for a given channel transconductance and its equivalent voltage, resulting in a bimodal sensing capability within a single device. This approach is effective because channel transconductance and its equivalent voltage are found to have a linear dependence on the temperature and pressure; thus, it is expected to serve as a general approach for the linear problem. Although it is not directly quantified, the improved gas sensing performance from the mechanical deformation seems to show a nonlinear relationship. A general strategy to overcome this grand challenge is still yet to come.

As volatile organic biomarkers often appear at ppb-level for practical applications toward healthcare, the detection of this ultra-low concentration is of significant interest. A well-established case is to diagnose the lung cancer with the biomarkers in the exhaled breath [151–153]. Toluene, one of the most common volatile organic biomarkers for lung cancer, is a suitable choice because of their significantly elevated levels in lung cancer patients [151]. When WO_3 nanofibers are decorated by Pd catalysts on both inner and outer layers, they show a low limit of toluene detection of 20 ppb in a simulated human exhaled breath at operating temperature of 350°C, suitable for diagnoses of lung cancer [152]. A low limit of detection as small as 2 ppb, as well as high response and good selectivity toward toluene, is also demonstrated by using the ordered mesoporous $NiFe_2O_4$ with the ultrathin framework and a large specific surface area [153]. Another representative example is to diagnose diabetes via ppb-level acetone detection in the human breath. A chemoresistive detector based on Si-doped WO_3 demonstrates an ultra-low acetone detection of 20 ppb, offering a potential for the noninvasive diagnosis of diabetes [47]. Despite great strides have been made in the ppb-level gas detection, challenges to detect this ultralow-level concentration of target gases in a complex environment at a fast, reliable, and cost-effective manner still need to be overcome to further promote the development of flexible and stretchable gas sensors for healthcare.

In addition, combining the wearable gas sensor with the other sensing modalities provides a comprehensive system for the healthcare, as demonstrated in several initial attempts. In addition to the example discussed in Section 4.3, a multisensor platform on a flexible plastic foil has been demonstrated to simultaneously measure oxidizing and reducing

gases, volatile organic compounds (VOCs), as well as humidity and temperature [154]. In such system integration, many practical issues will also need to be considered, including the high density of the active components or small footprint of the entire system, cost-effective manufacturing methods for large-scale production, high reliability and durability for long-term use, and others. Nonetheless, these grand challenges also represent a fraction of possibilities and opportunities for the research community. Due to the multidisciplinary nature of the burgeoning area of flexible and stretchable metal oxide gas sensors for healthcare, researchers from diverse fields are encouraged to work together to provide collective wisdom for additional discoveries in the future.

The work was supported by the start-up fund provided by the Engineering Science and Mechanics Department, College of Engineering, and Materials Research Institute at the Pennsylvania State University (PSU), the ASME Haythornthwaite Foundation Research Initiation Grant, and Dorothy Quiggle Career Development Professorship in Engineering and Global Engineering Leadership Program at PSU. The authors would like to thank the partial support from the National Natural Science Foundation of China (Grant No. 11572161) and State Key Laboratory for Strength and Vibration of Mechanical Structures (Grant No. SV2016-KF-17). The authors also would like to thank Mr. Han Li from Xiamen University for the helpful discussion and comments on this research.

1 Patel S, Park H, Bonato P, et al. A review of wearable sensors and systems with application in rehabilitation. J NeuroEng Rehabil, 2012, 9: 21
2 Trung T Q, Lee N E. Flexible and stretchable physical sensor integrated platforms for wearable human-activity monitoringand personal healthcare. Adv Mater, 2016, 28: 4338–4372
3 Cheng J P, Wang J, Li Q Q, et al. A review of recent developments in tin dioxide composites for gas sensing application. J Industrial Eng Chem, 2016, 44: 1–22
4 Mirzaei A, Leonardi S G, Neri G. Detection of hazardous volatile organic compounds (VOCs) by metal oxide nanostructures-based gas sensors: A review. Ceramics Int, 2016, 42: 15119–15141
5 Reid M, Reid R D, Oswal P, et al. NaDos: A real-time, wearable, personal exposure monitor for hazardous organic vapors. Senss Actuators B-Chem, 2018, 255: 2996–3003
6 Kahn N, Lavie O, Paz M, et al. Dynamic nanoparticle-based flexible sensors: Diagnosis of ovarian carcinoma from exhaled breath. Nano Lett, 2015, 15: 7023–7028
7 Yamada Y, Hiyama S, Toyooka T, et al. Ultratrace measurement of acetone from skin using zeolite: Toward development of a wearable monitor of fat metabolism. Anal Chem, 2015, 87: 7588–7594
8 Kim J, Valdés-Ramírez G, Bandodkar A J, et al. Non-invasive mouthguard biosensor for continuous salivary monitoring of metabolites. Analyst, 2014, 139: 1632–1636
9 Banday K M, Pasikanti K K, Chan E C Y, et al. Use of urine volatile organic compounds to discriminate tuberculosis patients from healthy subjects. Anal Chem, 2011, 83: 5526–5534
10 Alwis K U, Blount B C, Britt A S, et al. Simultaneous analysis of 28 urinary VOC metabolites using ultra high performance liquid chromatography coupled with electrospray ionization tandem mass spectrometry (UPLC-ESI/MSMS). Anal Chim Acta, 2012, 750: 152–160
11 Tricoli A, Nasiri N, De S. Wearable and miniaturized sensor technologies for personalized and preventive medicine. Adv Funct Mater, 2017, 27: 1605271
12 Feng F, Zheng J, Qin P, et al. A novel quartz crystal microbalance sensor array based on molecular imprinted polymers for simultaneous detection of clenbuterol and its metabolites. Talanta, 2017, 167: 94–102
13 Ding B, Kim J, Miyazaki Y, et al. Electrospun nanofibrous membranes coated quartz crystal microbalance as gas sensor for NH_3 detection. Senss Actuators B-Chem, 2004, 101: 373–380
14 Rana L, Gupta R, Kshetrimayum R, et al. Fabrication of surface acoustic wave based wireless NO_2 gas sensor. Surf Coatings Tech, 2018, 343: 89–92
15 Devkota J, Kim K J, Ohodnicki P R, et al. Zeolitic imidazolate framework-coated acoustic sensors for room temperature detection of carbon dioxide and methane. Nanoscale, 2018, 10: 8075–8087
16 Jildeh Z B, Oberländer J, Kirchner P, et al. Thermocatalytic behavior of manganese (IV) oxide as nanoporous material on the dissociation of a gas mixture containing hydrogen peroxide. Nanomaterials, 2018, 8: 262
17 Soltis R E. Zirconia-based electrochemical oxygen sensor for accurately determining water vapor concentration. ECS Trans, 2013, 50: 295–300
18 Ivers-Tiffée E, Härdtl K H, Menesklou W, et al. Principles of solid state oxygen sensors for lean combustion gas control. Electrochim Acta, 2001, 47: 807–814
19 Fahad H M, Shiraki H, Amani M, et al. Room temperature multiplexed gas sensing using chemical-sensitive 3.5-nm-thin silicon transistors. Sci Adv, 2017, 3: e1602557–9
20 Bohrer F I, Colesniuc C N, Park J, et al. Comparative gas sensing in cobalt, nickel, copper, zinc, and metal-free phthalocyanine chemiresistors. J Am Chem Soc, 2009, 131: 478–485
21 Marešová E, Tomeček D, Fitl P, et al. Textile chemiresistors with sensitive layers based on polymer ionic liquids: Applicability for detection of toxic gases and chemical warfare agents. Senss Actuators B-Chem, 2018, 266: 830–840
22 Bănică F G. Chemical Sensors and Biosensors: Fundamentals and Applications. John Wiley & Sons, 2012
23 Dey A. Semiconductor metal oxide gas sensors: A review. Mater Sci Eng-B, 2018, 229: 206–217
24 Hahn Y B, Ahmad R, Tripathy N. Chemical and biological sensors based on metal oxide nanostructures. Chem Commun, 2012, 48: 10369
25 Kim H J, Lee J H. Highly sensitive and selective gas sensors using p-type oxide semiconductors: Overview. Senss Actuators B-Chem, 2014, 192: 607–627
26 Rashid T R, Phan D T, Chung G S. A flexible hydrogen sensor based on Pd nanoparticles decorated ZnO nanorods grown on polyimide tape. Senss Actuators B-Chem, 2013, 185: 777–784
27 Ye Z, Jiang Y, Tai H, et al. The investigation of reduced graphene oxide@SnO_2–polyaniline composite thin films for ammonia detection at room temperature. J Mater Sci-Mater Electron, 2014, 26: 833–841
28 Singh G, Choudhary A, Haranath D, et al. ZnO decorated luminescent graphene as a potential gas sensor at room temperature. Carbon, 2012, 50: 385–394
29 Kim J W, Porte Y, Ko K Y, et al. Micropatternable double-faced ZnO nanoflowers for flexible gas sensor. ACS Appl Mater Interfaces, 2017, 9: 32876–32886
30 Liu J, Li S, Zhang B, et al. Ultrasensitive and low detection limit of nitrogen dioxide gas sensor based on flower-like ZnO hierarchical nanostructure modified by reduced graphene oxide. Senss Actuators B-Chem, 2017, 249: 715–724
31 Rui K, Wang X, Du M, et al. Dual-function metal–organic framework-based wearable fibers for gas probing and energy storage. ACS Appl Mater Interfaces, 2018, 10: 2837–2842
32 Lahlalia A, Filipovic L, Selberherr S. Modeling and simulation of novel semiconducting metal oxide gas sensors for wearable devices. IEEE Senss J, 2018, 18: 1960–1970

33 Park J, Kim J, Kim K, et al. Wearable, wireless gas sensors using highly stretchable and transparent structures of nanowires and graphene. Nanoscale, 2016, 8: 10591–10597
34 Comini E. Metal oxide nanowire chemical sensors: Innovation and quality of life. Mater Today, 2016, 19: 559–567
35 Hanf S, Bögözi T, Keiner R, et al. Fast and highly sensitive fiber-enhanced Raman spectroscopic monitoring of molecular H_2 and CH_4 for point-of-care diagnosis of malabsorption disorders in exhaled human breath. Anal Chem, 2014, 87: 982–988
36 Mridha S, Basak D. Investigation of a p-CuO/n-ZnO thin film heterojunction for H_2 gas-sensor applications. Semicond Sci Technol, 2006, 21: 928–932
37 Moon H G, Jung Y, Han S D, et al. Chemiresistive electronic nose toward detection of biomarkers in exhaled breath. ACS Appl Mater Interfaces, 2016, 8: 20969–20976
38 Zampetti E, Pantalei S, Muzyczuk A, et al. A high sensitive NO_2 gas sensor based on PEDOT–PSS/TiO_2 nanofibres. Senss Actuators B-Chem, 2013, 176: 390–398
39 Vreman H J, Stevenson D K, Oh W, et al. Semiportable electrochemical instrument for determining carbon monoxide in breath. Clin Chem, 1994, 40: 1927–1933
40 Bârsan N, Weimar U. Understanding the fundamental principles of metal oxide based gas sensors: The example of CO sensing with SnO_2 sensors in the presence of humidity. J Phys Condens Mat, 2003, 15: R813
41 Chatterjee M, Ge X, Kostov Y, et al. A rate-based transcutaneous CO_2 sensor for noninvasive respiration monitoring. Physiol Meas, 2015, 36: 883–894
42 Gouma P, Kalyanasundaram K, Yun X, et al. Nanosensor and breath analyzer for ammonia detection in exhaled human breath. IEEE Senss J, 2010, 10: 49–53
43 Sun C, Dutta P K. Selective detection of part per billion concentrations of ammonia using a p–n semiconducting oxide heterostructure. Senss Actuators B-Chem, 2016, 226: 156–169
44 Arena A, Donato N, Saitta G, et al. Flexible ethanol sensors on glossy paper substrates operating at room temperature. Senss Actuators B-Chem, 2010, 145: 488–494
45 Zhan S, Li D, Liang S, et al. A novel flexible room temperature ethanol gas sensor based on SnO_2 doped poly-diallyldimethylammonium chloride. Sensors, 2013, 13: 4378–4389
46 Righettoni M, Tricoli A. Toward portable breath acetone analysis for diabetes detection. J Breath Res, 2011, 5: 037109
47 Righettoni M, Tricoli A, Pratsinis S E. Si:WO_3 sensors for highly selective detection of acetone for easy diagnosis of diabetes by breath analysis. Anal Chem, 2010, 82: 3581–3587
48 Franke M E, Koplin T J, Simon U. Metal and metal oxide nanoparticles in chemiresistors: Does the nanoscale matter? Small, 2006, 2: 36–50
49 Barsan N, Koziej D, Weimar U. Metal oxide-based gas sensor research: How to? Senss Actuators B-Chem, 2007, 121: 18–35
50 Weisz P B. Effects of electronic charge transfer between adsorbate and solid on chemisorption and catalysis. J Chem Phys, 1953, 21: 1531–1538
51 Madou M J, Morrison S R. Chemical sensing with solid state devices. Elsevier, 1989
52 Bag A K, Tudu B, Roy J, et al. Optimization of sensor array in electronic nose: A rough set-based approach. IEEE Senss J, 2011, 11: 3001–3008
53 Miller D R, Akbar S A, Morris P A. Corrigendum to nanoscale metal oxide-based heterojunctions for gas sensing: A review. Senss Actuators B-Chem, 2015, 211: 569–570
54 Uddin A S M I, Yaqoob U, Phan D T, et al. A novel flexible acetylene gas sensor based on PI/PTFE-supported Ag-loaded vertical ZnO nanorods array. Senss Actuators B-Chem, 2016, 222: 536–543
55 Comini E. Integration of metal oxide nanowires in flexible gas sensing devices. Sensors, 2013, 13: 10659–10673
56 Nadarajah A, Word R C, Meiss J, et al. Flexible inorganic nanowire light-emitting diode. Nano Lett, 2008, 8: 534–537
57 Ahn H, Park J H, Kim S B, et al. Vertically aligned ZnO nanorod sensor on flexible substrate for ethanol gas monitoring. Electrochem Solid-State Lett, 2010, 13: J125
58 Shim J B, Kim H S, Chang H, et al. Growth and optical properties of aluminum-doped zinc oxide nanostructures on flexible substrates in flexible electronics. J Mater Sci-Mater Electron, 2011, 22: 1350–1356
59 Manekkathodi A, Lu M Y, Wang C W, et al. Direct growth of aligned zinc oxide nanorods on paper substrates for low-cost flexible electronics. Adv Mater, 2010, 22: 4059–4063
60 Gullapalli H, Vemuru V S M, Kumar A, et al. Flexible piezoelectric ZnO-paper nanocomposite strain sensor. Small, 2010, 6: 1641–1646
61 Artzi-Gerlitz R, Benkstein K D, Lahr D L, et al. Fabrication and gas sensing performance of parallel assemblies of metal oxide nanotubes supported by porous aluminum oxide membranes. Senss Actuators B-Chem, 2009, 136: 257–264
62 Zang W, Nie Y, Zhu D, et al. Core–Shell In_2O_3/ZnO nanoarray nanogenerator as a self-powered active gas sensor with high H_2S sensitivity and selectivity at room temperature. J Phys Chem C, 2014, 118: 9209–9216
63 Bai S, Tian Y, Cui M, et al. Polyaniline@SnO_2 heterojunction loading on flexible PET thin film for detection of NH_3 at room temperature. Senss Actuators B-Chem, 2016, 226: 540–547
64 Yi J, Lee J M, Park W I. Vertically aligned ZnO nanorods and graphene hybrid architectures for high-sensitive flexible gas sensors. Senss Actuators B-Chem, 2011, 155: 264–269
65 Zhou J, Xu N , Wang Z . Dissolving behavior and stability of ZnO wires in biofluids: A study on biodegradability and biocompatibility of ZnO nanostructures. Adv Mater, 2006, 18: 2432–2435
66 Zappa D, Comini E, Zamani R, et al. Preparation of copper oxide nanowire-based conductometric chemical sensors. Senss Actuators B-Chem, 2013, 182: 7–15
67 Mema R, Yuan L, Du Q, et al. Effect of surface stresses on CuO nanowire growth in the thermal oxidation of copper. Chem Phys Lett, 2011, 512: 87–91
68 Deshpande N G, Gudage Y G, Sharma R, et al. Studies on tin oxide-intercalated polyaniline nanocomposite for ammonia gas sensing applications. Senss Actuators B-Chem, 2009, 138: 76–84
69 Prasad A K, Kubinski D J, Gouma P I. Comparison of sol–gel and ion beam deposited MoO_3 thin film gas sensors for selective ammonia detection. Senss Actuators B-Chem, 2003, 93: 25–30
70 Yaqoob U, Phan D T, Uddin A S M I, et al. Highly flexible room temperature NO_2 sensor based on MWCNTs-WO_3 nanoparticles hybrid on a PET substrate. Senss Actuators B-Chem, 2015, 221: 760–768
71 Karunagaran B, Uthirakumar P, Chung S J, et al. TiO_2 thin film gas sensor for monitoring ammonia. Mater Charact, 2007, 58: 680–684
72 Perillo P M, Rodríguez D F. Low temperature trimethylamine flexible gas sensor based on TiO_2 membrane nanotubes. J Alloys Compd, 2016, 657: 765–769
73 Li S, Lin P, Zhao L, et al. The room temperature gas sensor based on polyaniline@flower-like WO_3 nanocomposites and flexible PET substrate for NH_3 detection. Senss Actuators B-Chem, 2018, 259: 505–513
74 Galstyan V, Vomiero A, Comini E, et al. TiO_2 nanotubular and nanoporous arrays by electrochemical anodization on different substrates. RSC Adv, 2011, 1: 1038–1044
75 Galstyan V, Comini E, Vomiero A, et al. Fabrication of pure and Nb–TiO_2 nanotubes and their functional properties. J Alloys Compd, 2012, 536: S488–S490
76 Fan Z, Ho J C, Takahashi T, et al. Toward the development of printable nanowire electronics and sensors. Adv Mater, 2009, 21: 3730–3743
77 Carlson A, Bowen A M, Huang Y, et al. Transfer printing techniques for materials assembly and micro/nanodevice fabrication. Adv Mater, 2012, 24: 5284–5318

78 Gao Y, Cheng H. Assembly of heterogeneous materials for biology and electronics: From bio-inspiration to bio-integration. J Electron Packag, 2017, 139: 020801
79 Yu Q, Chen F, Zhou H, et al. Design and analysis of magnetic-assisted transfer printing. J Appl Mech, 2018, 85: 101009
80 Jeong H Y, Lee D S, Choi H K, et al. Flexible room-temperature NO_2 gas sensors based on carbon nanotubes/reduced graphene hybrid films. Appl Phys Lett, 2010, 96: 213105
81 Kumaresan Y, Lee R, Lim N, et al. Extremely flexible indium-gallium-zinc oxide (IGZO) based electronic devices placed on an ultrathin poly(methyl methacrylate) (PMMA) substrate. Adv Electron Mater, 2018, 4: 1800167
82 Zheng Z Q, Yao J D, Wang B, et al. Light-controlling, flexible and transparent ethanol gas sensor based on ZnO nanoparticles for wearable devices. Sci Rep, 2015, 5: 11070
83 Choi S J, Choi H J, Koo W T, et al. Metal–organic framework-templated PdO-Co_3O_4 nanocubes functionalized by SWCNTs: Improved NO_2 reaction kinetics on flexible heating film. ACS Appl Mater Interfaces, 2017, 9: 40593–40603
84 McAlpine M C, Ahmad H, Wang D, et al. Highly ordered nanowire arrays on plastic substrates for ultrasensitive flexible chemical sensors. Nat Mater, 2007, 6: 379–384
85 Geng C, Jiang Y, Yao Y, et al. Well-aligned ZnO nanowire arrays fabricated on silicon substrates. Adv Funct Mater, 2004, 14: 589–594
86 Duan X, Niu C, Sahi V, et al. High-performance thin-film transistors using semiconductor nanowires and nanoribbons. Nature, 2003, 425: 274–278
87 Huang Y, Duan X, Wei Q, et al. Directed assembly of one-dimensional nanostructures into functional networks. Science, 2001, 291: 630–633
88 Li X, Zhang L, Wang X, et al. Langmuir−Blodgett assembly of densely aligned single-walled carbon nanotubes from bulk materials. J Am Chem Soc, 2007, 129: 4890–4891
89 Jin S, Whang D, McAlpine M C, et al. Scalable interconnection and integration of nanowire devices without registration. Nano Lett, 2004, 4: 915–919
90 Tao A, Kim F, Hess C, et al. Langmuir−Blodgett silver nanowire monolayers for molecular sensing using surface-enhanced Raman spectroscopy. Nano Lett, 2003, 3: 1229–1233
91 Yu G, Cao A, Lieber C M. Large-area blown bubble films of aligned nanowires and carbon nanotubes. Nat Nanotech, 2007, 2: 372–377
92 Dong L, Bush J, Chirayos V, et al. Dielectrophoretically controlled fabrication of single-crystal nickel silicide nanowire interconnects. Nano Lett, 2005, 5: 2112–2115
93 Englander O, Christensen D, Kim J, et al. Electric-field assisted growth and self-assembly of intrinsic silicon nanowires. Nano Lett, 2005, 5: 705–708
94 Takahashi T, Takei K, Ho J C, et al. Monolayer resist for patterned contact printing of aligned nanowire arrays. J Am Chem Soc, 2009, 131: 2102–2103
95 Fan Z, Ho J C, Jacobson Z A, et al. Large-scale, heterogeneous integration of nanowire arrays for image sensor circuitry. Proc Natl Acad Sci USA, 2008, 105: 11066–11070
96 Fan Z, Ho J C, Jacobson Z A, et al. Wafer-scale assembly of highly ordered semiconductor nanowire arrays by contact printing. Nano Lett, 2008, 8: 20–25
97 Yao J, Yan H, Lieber C M. A nanoscale combing technique for the large-scale assembly of highly aligned nanowires. Nat Nanotech, 2013, 8: 329–335
98 Ishikawa F N, Chang H K, Ryu K, et al. Transparent electronics based on transfer printed aligned carbon nanotubes on rigid and flexible substrates. ACS Nano, 2009, 3: 73–79
99 Chen P C, Sukcharoenchoke S, Ryu K, et al. 2,4,6-Trinitrotoluene (TNT) chemical sensing based on aligned single-walled carbon nanotubes and ZnO nanowires. Adv Mater, 2010, 22: 1900–1904
100 Huang H, Liang B, Liu Z, et al. Metal oxide nanowire transistors. J Mater Chem, 2012, 22: 13428–13445
101 Lim Z H, Chia Z X, Kevin M, et al. A facile approach towards ZnO nanorods conductive textile for room temperature multifunctional sensors. Senss Actuators B-Chem, 2010, 151: 121–126
102 Kinkeldei T, Zysset C, Münzenrieder N, et al. An electronic nose on flexible substrates integrated into a smart textile. Senss Actuators B-Chem, 2012, 174: 81–86
103 Subbiah D K, Mani G K, Babu K J, et al. Nanostructured ZnO on cotton fabrics–A novel flexible gas sensor & UV filter. J Cleaner Production, 2018, 194: 372–382
104 Yang A, Tao X, Wang R, et al. Room temperature gas sensing properties of SnO_2/multiwall-carbon-nanotube composite nanofibers. Appl Phys Lett, 2007, 91: 133110
105 Tonezzer M, Lacerda R G. Zinc oxide nanowires on carbon microfiber as flexible gas sensor. Physica E-Low-dimensional Syst NanoStruct, 2012, 44: 1098–1102
106 Kim D H, Rogers J A. Stretchable electronics: Materials strategies and devices. Adv Mater, 2008, 20: 4887–4892
107 Rogers J A, Someya T, Huang Y. Materials and mechanics for stretchable electronics. Science, 2010, 327: 1603–1607
108 Cheng H, Yi N. Dissolvable tattoo sensors: From science fiction to a viable technology. Phys Scr, 2017, 92: 013001
109 Zhu J, Dexheimer M, Cheng H. Reconfigurable systems for multifunctional electronics. npj Flex Electron, 2017, 1: 8
110 Khang D Y, Jiang H, Huang Y, et al. A stretchable form of single-crystal silicon for high-performance electronics on rubber substrates. Science, 2006, 311: 208–212
111 Cheng H, Song J. A simply analytic study of buckled thin films on compliant substrates. J Appl Mech, 2013, 81: 024501
112 Cheng H, Zhang Y, Hwang K C, et al. Buckling of a stiff thin film on a pre-strained bi-layer substrate. Int J Solids Struct, 2014, 51: 3113–3118
113 Kim D H, Song J, Mook Choi W, et al. Materials and noncoplanar mesh designs for integrated circuits with linear elastic responses to extreme mechanical deformations. Proc Natl Acad Sci USA, 2008, 105: 18675–18680
114 Xu S, Zhang Y, Cho J, et al. Stretchable batteries with self-similar serpentine interconnects and integrated wireless recharging systems. Nat Commun, 2013, 4: 1543
115 Zhang Y, Fu H, Su Y, et al. Mechanics of ultra-stretchable self-similar serpentine interconnects. Acta Mater, 2013, 61: 7816–7827
116 Yu Q, Chen F, Li M, et al. Buckling analysis of stiff thin films suspended on a substrate with tripod surface relief structure. Appl Phys Lett, 2017, 111: 121904
117 Cheng H, Wu J, Li M, et al. An analytical model of strain isolation for stretchable and flexible electronics. Appl Phys Lett, 2011, 98: 061902
118 Lee J, Wu J, Shi M, et al. Stretchable GaAs photovoltaics with designs that enable high areal coverage. Adv Mater, 2011, 23: 986–991
119 Liu Z, Cheng H, Wu J. Mechanics of solar module on structured substrates. J Appl Mech, 2014, 81: 064502
120 Kang D, Pikhitsa P V, Choi Y W, et al. Ultrasensitive mechanical crack-based sensor inspired by the spider sensory system. Nature, 2014, 516: 222–226
121 Liu Z, Yu M, Lv J, et al. Dispersed, porous nanoislands landing on stretchable nanocrack gold films: Maintenance of stretchability and controllable impedance. ACS Appl Mater Interfaces, 2014, 6: 13487–13495
122 Won Y, Kim A, Yang W, et al. A highly stretchable, helical copper nanowire conductor exhibiting a stretchability of 700%. NPG Asia Mater, 2014, 6: e132
123 Xu S, Yan Z, Jang K I, et al. Assembly of micro/nanomaterials into complex, three-dimensional architectures by compressive buckling. Science, 2015, 347: 154–159
124 Song Z, Ma T, Tang R, et al. Origami lithium-ion batteries. Nat Commun, 2014, 5: 3140
125 Yan Z, Zhang F, Wang J, et al. Controlled mechanical buckling for

origami-inspired construction of 3D microstructures in advanced materials. Adv Funct Mater, 2016, 26: 2629–2639
126 Blees M K, Barnard A W, Rose P A, et al. Graphene kirigami. Nature, 2015, 524: 204–207
127 Song Z, Wang X, Lv C, et al. Kirigami-based stretchable lithium-ion batteries. Sci Rep, 2015, 5: 10988
128 Park J, Lee Y, Hong J, et al. Tactile-direction-sensitive and stretchable electronic skins based on human-skin-inspired interlocked microstructures. ACS Nano, 2014, 8: 12020–12029
129 Ha M, Lim S, Park J, et al. Bioinspired interlocked and hierarchical design of ZnO nanowire arrays for static and dynamic pressure-sensitive electronic skins. Adv Funct Mater, 2015, 25: 2841–2849
130 Song Z, Huang Z, Liu J, et al. Fully stretchable and humidity-resistant quantum dot gas sensors. ACS Sens, 2018, 3: 1048–1055
131 Song Z, Xu S, Liu J, et al. Enhanced catalytic activity of SnO_2 quantum dot films employing atomic ligand-exchange strategy for fast response H_2S gas sensors. Senss Actuators B-Chem, 2018, 271: 147–156
132 Kim D, Kim D, Lee H, et al. Body-attachable and stretchable multisensors integrated with wirelessly rechargeable energy storage devices. Adv Mater, 2016, 28: 748–756
133 Gutruf P, Zeller E, Walia S, et al. Stretchable and tunable microtectonic ZnO-based sensors and photonics. Small, 2015, 11: 4532–4539
134 Liao X, Liao Q, Zhang Z, et al. A highly stretchable ZnO@fiber-based multifunctional nanosensor for strain/temperature/UV detection. Adv Funct Mater, 2016, 26: 3074–3081
135 Gutruf P, Shah C M, Walia S, et al. Transparent functional oxide stretchable electronics: Micro-tectonics enabled high strain electrodes. NPG Asia Mater, 2013, 5
136 Mishra Y K, Kaps S, Schuchardt A, et al. Fabrication of macroscopically flexible and highly porous 3D semiconductor networks from interpenetrating nanostructures by a simple flame transport approach. Part Part Syst Charact, 2013, 30: 775–783
137 Paulowicz I, Hrkac V, Kaps S, et al. Three-dimensional SnO_2 nanowire networks for multifunctional applications: From high-temperature stretchable ceramics to ultraresponsive sensors. Adv Electron Mater, 2015, 1: 1500081
138 Zhang R Q, Lifshitz Y, Lee S T. Oxide-assisted growth of semiconducting nanowires. Adv Mater, 2003, 15: 635–640
139 Wang Z L. Nanobelts, nanowires, and nanodiskettes of semiconducting oxides—From materials to nanodevices. Adv Mater, 2003, 15: 432–436
140 Liu H, Li M, Voznyy O, et al. Physically flexible, rapid-response gas sensor based on colloidal quantum dot solids. Adv Mater, 2014, 26: 2718–2724
141 Song Z, Wei Z, Wang B, et al. Sensitive room-temperature H_2S gas sensors employing SnO_2 quantum wire/reduced graphene oxide nanocomposites. Chem Mater, 2016, 28: 1205–1212
142 Prades J D, Jimenez-Diaz R, Hernandez-Ramirez F, et al. Harnessing self-heating in nanowires for energy efficient, fully autonomous and ultra-fast gas sensors. Senss Actuators B-Chem, 2010, 144: 1–5
143 Prades J D, Jimenez-Diaz R, Hernandez-Ramirez F, et al. Ultralow power consumption gas sensors based on self-heated individual nanowires. Appl Phys Lett, 2008, 93: 123110
144 Prades J D, Jimenez-Diaz R, Hernandez-Ramirez F, et al. Equivalence between thermal and room temperature UV light-modulated responses of gas sensors based on individual SnO_2 nanowires. Senss Actuators B-Chem, 2009, 140: 337–341
145 Law M, Kind H, Messer B, et al. Photochemical sensing of NO_2 with SnO_2 nanoribbon nanosensors at room temperature. Angew Chem Int Ed, 2002, 41: 2405–2408
146 Comini E, Faglia G, Sberveglieri G. UV light activation of tin oxide thin films for NO_2 sensing at low temperatures. Senss Actuators B-Chem, 2001, 78: 73–77
147 Comini E, Ottini L, Faglia G, et al. light activation of tin oxide thin films for UV activation for CO monitoring. IEEE Senss J, 2004, 4: 17–20
148 Comini E, Cristalli A, Faglia G, et al. Light enhanced gas sensing properties of indium oxide and tin dioxide sensors. Senss Actuators B-Chem, 2000, 65: 260–263
149 de Lacy Costello B P J, Ewen R J, Ratcliffe N M, et al. Highly sensitive room temperature sensors based on the UV-LED activation of zinc oxide nanoparticles. Senss Actuators B-Chem, 2008, 134: 945–952
150 Tien N T, Jeon S, Kim D I, et al. A flexible bimodal sensor array for simultaneous sensing of pressure and temperature. Adv Mater, 2014, 26: 796–804
151 Peng G, Tisch U, Adams O, et al. Diagnosing lung cancer in exhaled breath using gold nanoparticles. Nat Nanotech, 2009, 4: 669–673
152 Kim N H, Choi S J, Yang D J, et al. Highly sensitive and selective hydrogen sulfide and toluene sensors using Pd functionalized WO_3 nanofibers for potential diagnosis of halitosis and lung cancer. Senss Actuators B-Chem, 2014, 193: 574–581
153 Lai X, Cao K, Shen G, et al. Ordered mesoporous $NiFe_2O_4$ with ultrathin framework for low-ppb toluene sensing. Sci Bull, 2018, 63: 187–193
154 Oprea A, Courbat J, Briand D, et al. Environmental monitoring with a multisensor platform on polyimide foil. Senss Actuators B-Chem, 2012, 171–172: 190–197